

Field induced spin reorientation and giant spin-lattice coupling in EuFe_2As_2

Y. Xiao,^{1,*} Y. Su,² W. Schmidt,³ K. Schmalzl,³ C.M.N. Kumar,¹ S. Price,¹ T. Chatterji,³ R. Mittal,^{2,4}
L. J. Chang,⁵ S. Nandi,¹ N. Kumar,⁶ S. K. Dhar,⁶ A. Thamizhavel,⁶ and Th. Brueckel^{1,2,3}

¹*Institut fuer Festkoerperforschung, Forschungszentrum Juelich, D-52425 Juelich, Germany*

²*Juelich Centre for Neutron Science, IFF, Forschungszentrum Juelich,
Outstation at FRM II, Lichtenbergstr. 1, D-85747 Garching, Germany*

³*Juelich Centre for Neutron Science, IFF, Forschungszentrum Juelich,
Outstation at Institut Laue-Langevin, BP 156, 38042 Grenoble Cedex 9, France*

⁴*Solid State Physics Division, Bhabha Atomic Research Centre, Trombay, Mumbai 400 085, India*

⁵*Nuclear Science and Technology Development Center,
National Tsing Hua University, Hsinchu 30013, Taiwan*

⁶*Department of Condensed Matter Physics and Material Sciences,
Tata Institute of Fundamental Research, Homi Bhabha Road, Colaba, Mumbai 400 005, India*

(Dated: March 31, 2010)

We have studied a EuFe_2As_2 single crystal by neutron diffraction under magnetic fields up to 3.5 T and temperatures down to 2 K. A field induced spin reorientation is observed in the presence of a magnetic field along both the a and c axes, respectively. Above critical field, the ground state antiferromagnetic configuration of Eu^{2+} moments transforms into a ferromagnetic structure with moments along the applied field direction. The magnetic phase diagram for Eu magnetic sublattice in EuFe_2As_2 is presented. A considerable strain ($\sim 0.9\%$) is induced by the magnetic field, caused by the realignment of the twinning structure. Furthermore, the realignment of the twinning structure is found to be reversible with the rebound of magnetic field, which suggested the existence of magnetic shape-memory effect. The Eu moment ordering exhibits close relationship with the twinning structure. We argue that the Zeeman energy in combined with magnetic anisotropy energy is responsible for the observed spin-lattice coupling.

PACS numbers: 74.70.Xa, 75.25.-j, 75.30.Kz, 75.80.+q

The recent discovery of iron pnictide superconductors has triggered extensive research on their physical properties and mechanism of high temperature superconductors [1–3]. All iron pnictides are found to be of layered structure in nature. For undoped iron pnictides, the chains of parallel Fe spins within the FeAs layers couple antiferromagnetically in the ab plane of the orthorhombic lattice with an antiparallel arrangement along the c axis [4–6]. This antiferromagnetic (AFM) order in the parent compounds is likely due to a spin-density-wave (SDW) instability caused by Fermi surface nesting [7]. Similar to the high T_c cuprate superconductors, the undoped iron pnictides are not superconducting under ambient pressure and show an antiferromagnetic SDW order. Upon carrier doping, the magnetic order is suppressed and superconductivity emerges concomitantly [8, 9].

EuFe_2As_2 is a peculiar member of the iron arsenide AFe_2As_2 family since the A site is occupied by Eu^{2+} , which is an S -state (orbital angular momentum $L = 0$) rare-earth ion possessing a $4f^7$ structure with the total electron spin $S = 7/2$. The theoretical effective magnetic moment of Eu^{2+} ion is $7.94 \mu_B$. Our previous neutron diffraction work on EuFe_2As_2 single crystals revealed that the Fe and Eu spins form long range AFM order below 190 and 19 K, respectively [10]. Furthermore, early studies have shown that an external magnetic field may induce ferromagnetic (FM) order in EuFe_2As_2 [11], which suggested a weak AFM coupling between Eu spins. The superconductivity can be achieved by applying high pressure or doping on either Eu or As site in EuFe_2As_2 [12–15]. Interestingly, some works show that the ordering of the

Eu^{2+} moments persisted in the superconducting phase, such as in the pressure-induced EuFe_2As_2 superconductor [12] and $\text{EuFe}_2(\text{As}_{0.7}\text{P}_{0.3})_2$ superconductor [13]. However, the role of Eu magnetism in superconductivity is not yet clear and the Eu ordering state in different systems still need to be clarified.

Here we report a single crystal neutron diffraction measurement on EuFe_2As_2 under a magnetic field up to 3.5 T. The spin reorientation of Eu moments is observed upon an applied magnetic field parallel to both a and c axes of the orthorhombic structure, while the Fe SDW order persists at high magnetic fields. Interestingly, the application of a magnetic field changes the twinning population in EuFe_2As_2 and the redistribution of the domain population is found to be associated with the evolution of the magnetic order of Eu moments, which indicates the existence of a giant spin-lattice coupling effect. A single crystal of EuFe_2As_2 was grown by the Sn-flux method [10]. It was in shape of a platelet with approximate dimensions of $5 \times 5 \times 1 \text{ mm}^3$. Single crystal neutron scattering measurements were performed on the thermal neutron two-axis diffractometer D23 at the Institut Laue Langevin (Grenoble, France). To investigate the evolution of the magnetic order of EuFe_2As_2 under magnetic field, the crystal was aligned in the a - c scattering plane and a horizontal magnetic field up to 3.5 T was applied by using a cryomagnet. The measurement was performed with an incident neutron wavelength of 1.28 \AA .

In zero field, the crystal structure of EuFe_2As_2 can be well described within the orthorhombic symmetry at 2 K and the magnetic reflections originated from both Eu and Fe magnetic sublattices were observed. The long range ordering of Eu^{2+}

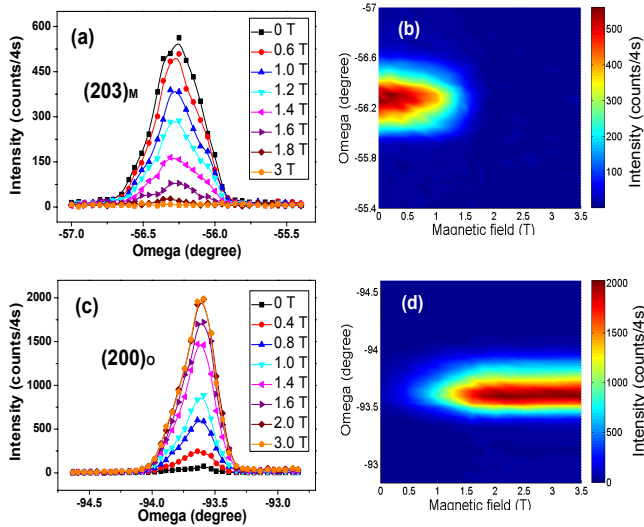


FIG. 1: (Color online) (a) Evolution of $(203)_M$ magnetic reflections with the change of magnetic field at 2 K. (b) Magnetic field dependence of $(203)_M$ magnetic reflection in two dimensional plot. (c) Evolution of $(200)_O$ reflection with the change of magnetic field at 2 K. (d) Magnetic field dependence of $(200)_O$ reflections in two dimensional plot.

[with $\mathbf{k} = (0,0,1)$] and Fe^{2+} moments [with $\mathbf{k} = (1,0,1)$] forms a AFM structure as confirmed in our previous neutron diffraction study [10]. Several typical AFM reflections of the Eu ordering, such as $(201)_M$, $(203)_M$ and $(005)_M$, were selected to examine the magnetic structure evolution under the magnetic field (H) along both c and a axes, i.e. $[001]$ and $[100]$ directions, respectively. As an example, the field dependence of the $(203)_M$ reflection is plotted in Fig. 1(a) and Fig. 1(b) in two dimensions. Application of an field along c axis strongly weakens the $(203)_M$ reflection and suppresses it totally at the critical field ($H_{\text{Crit}}^{\text{Eu}}$) of 1.8 T at 2 K. On the other hand, the increase of intensity at some nuclear reflection positions, e.g. $(200)_O$ as shown in Fig. 1(c) and (d), indicates that the Eu spin gradually reorientate from the ab plane to the $[001]$ direction. The field-induced magnetic phase transition takes place from antiferromagnetic, via a canted configuration, to the ferromagnetic structure. Note that the small nuclear structure factor of the $(200)_O$ reflection makes it possible for us to clearly observe the contribution from magnetic scattering.

Fig. 2.(a) and (b) display the field dependence of integrated intensities of selected magnetic scattering reflections in EuFe_2As_2 with the field parallel to the c axis at different temperatures. The critical field at which the Eu magnetic order changes from AFM to FM is decreasing with increasing temperature. When the field is parallel to the a axis, it is observed that the intensity of the $(201)_M$ reflection increases slightly and then decrease sharply with increasing strength of the applied field at 2 K [see Fig. 2(c)]. It is known that diffraction signals from both $(201)_M$ and $(021)_M$ reflections will be detected due to the twinning configuration [10]. The initial increase of the $(201)_M$ intensity in Fig. 2(c) is caused by the

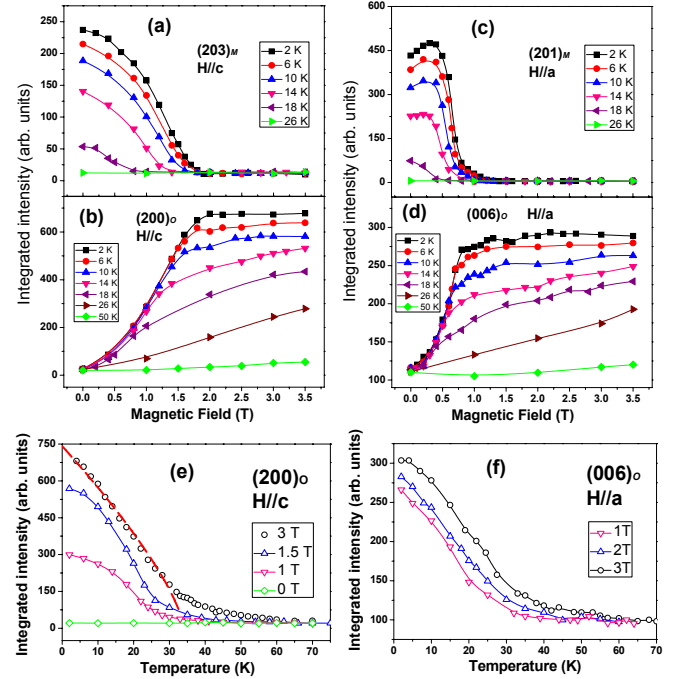


FIG. 2: (Color online) (a)(b) Integrated intensity of $(203)_M$ and $(200)_O$ reflections as a function of magnetic field with the field applied parallel to c axis. (c)(d) Magnetic field dependence of integrated intensity of $(201)_M$ and $(006)_O$ reflections at different temperatures with the magnetic field applied parallel to a axis. (e)(f) Temperature dependence of integrated intensity of $(200)_O$ and $(006)_O$ reflections.

increasing contribution from the $(021)_M$ reflection, which is related to the rotation of the $(0k0)$ domains. Actually, the redistribution of domains under an applied field is observed and it will be discussed in the following text. In Fig. 2(d), the increase in the intensities of the $(00l)$ reflections with l even is observed instead of the $(h00)$ reflections. All these results suggest that the Eu spins will orient to the direction of the applied magnetic field once the field strength is greater than the critical field. The FM arrangement of Eu spins is further confirmed by the refinement of the reflections collected under the field of 3 T at 2 K. The amplitude of Eu moment is estimated to be $6.9(4) \mu_B$ and $6.7(4) \mu_B$ for the two FM structures with Eu moments along the c and a axis, respectively. The temperature dependence of FM reflections was measured afterwards to determine the ordering temperature of the Eu moments. Fig. 2(e) and (f) show the temperature evolution of integrated intensities of the $(200)_O$ and $(006)_O$ Bragg reflections for H parallel to c and a axes, respectively. A power-law was adopted to describe this second order transition by fitting the temperature variation in the ordering parameters. As indicated by the dash line, the power-law fit on the data at 3 T in Fig. 2.(e) yields a magnetic ordering transition temperature $T_C = 33.5(4)$ K. The intensity tail above T_C is caused by the contribution from the field induced moment. According to the neutron measurement results, the magnetic phase transition temperatures are determined and plotted in Fig. 3(a) and

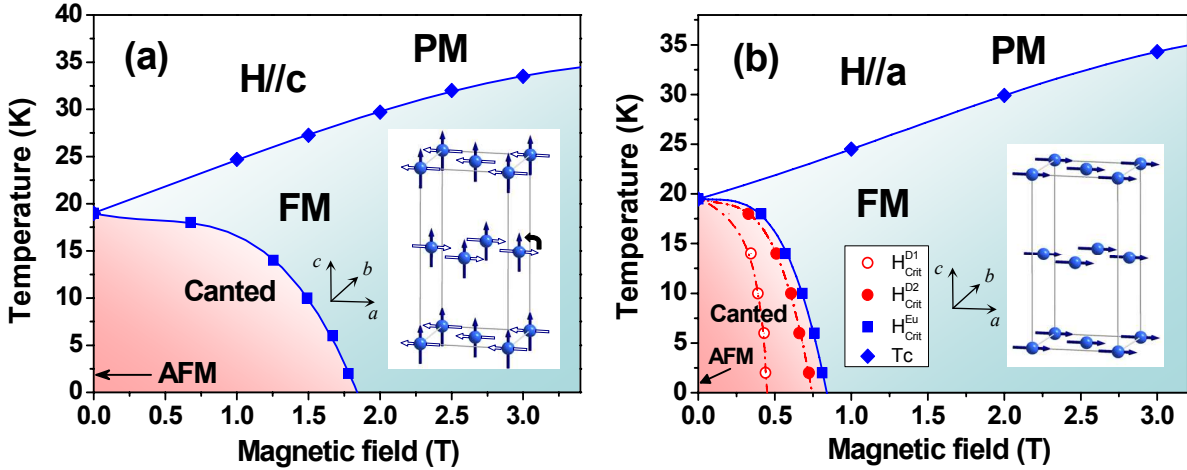


FIG. 3: (Color online) (a) Magnetic phase diagram for EuFe_2As_2 with applied field parallel to the crystallographic c axis. The inset shows the schematic view of the magnetic structure. The AFM magnetic structure at zero field is denoted as the open arrows, while the field induced FM structure is denoted as the solid one. (b) Magnetic phase diagram for EuFe_2As_2 with applied field parallel to the crystallographic a axis. The lines are guide to the eye. See text for more details.

(b). It can be seen that the application of a magnetic field not only changes the ordering configuration but also enhances the ordering temperature of the Eu moment.

Besides of Eu order, we also examined the Fe order under the applied field along both c and a axes. In contrast to the reorientation of the Eu spins, the AFM SDW order of Fe is found to be robust and it persists till fields up to 3 T. The two dimensional plot of the $(101)_M$ reflection under a 3 T field at 2 K is shown in Fig. 4(a). Surprisingly, it is found that the integrated intensity of the $(101)_M$ magnetic reflection decreases slightly and then sharply increases with increasing magnetic field, as shown in Fig. 4(b). As we know that a twinning structure may exist in orthorhombic EuFe_2As_2 phase due to the interchange of the orthorhombic a and b axes. Additionally, the intensity of the $(101)_M$ reflection only originates from the magnetic scattering of the $(h00)$ twin. In order to clarify the evolution of twinning structure under applied field, the $(400)_O$ reflection was examined from zero field up to 3.5 T since both $(040)_O$ and $(400)_O$ reflections measured in present magnetic structural configuration are pure nuclear reflections. As shown in Fig. 4(c), the twinning structure forms at zero field and results in the splitting between the $(400)_O$ and $(040)_O$ reflections. The domain population is estimated to be 1:3 for the $(h00)$ and $(0k0)$ twins at zero field. It is interesting that only the $(400)_O$ reflection is observed when the magnetic field is increased up to 3 T [Fig. 4(d)]. The single reflection from $(400)_O$ is further confirmed by carefully checking the vicinity in reciprocal space, which indicates that the single crystal is detwinned. The detailed evolution of the domain population with increasing field is illustrated by the intensity change of the $(400)_O$ and $(040)_O$ reflections [Fig. 4(e)]. With increasing field, the intensity of the $(400)_O$ decreases slowly and reaches the lowest at the critical field H_{Crit}^{D1} and suddenly increases at the higher critical

field H_{Crit}^{D2} . Whereas the $(040)_O$ reflection vanishes at H_{Crit}^{D2} in the other hand. Therefore, H_{Crit}^{D2} can be considered as the critical field at which the $(0k0)$ domains overcome the domain wall energy and realign to $(h00)$ domains. The realignment of the $(0k0)$ domains will firstly introduce internal stress and this stress will act on the $(h00)$ domains and tilt them slightly away from the balance position, which leads to the decrease of the $(400)_O$ reflection. However, $(h00)$ domains will rebound to the balance position when the $(0k0)$ domains realign to the $(h00)$ domains. Therefore, H_{Crit}^{D1} corresponds to the critical field when the $(h00)$ domains tilted and formed the largest tilting angle away from the balance position. The Q -scans of the $(400)_O$ reflection under three typical fields are plotted in Fig. 4(f). Based on the peak position of the $(400)_O$ and $(040)_O$ reflections, the strain caused by the twin boundary motion was estimated to be around 0.9%. In contrast with some magnetic shape-memory alloy, where the field induced strains are associated with the martensite/austenite phase transition [16, 17], the field induced strains in the present EuFe_2As_2 single crystal is caused by the domain realignment purely. Furthermore, it is observed that the realignment of domains is a reversible process with a rebound field, as shown in Fig. 4(c).

The critical fields H_{Crit}^{D1} and H_{Crit}^{D2} are also determined at different temperatures and plotted in Fig. 3 as the red circles and dots. It is interesting that the critical field of the domain redistribution is closely correlated with the field that induces the AFM-FM transition of the Eu magnetic sublattice. The energy difference between two domains seems strongly related with the total energy of the Eu magnetism. Usually, the application of mechanical compressive stress σ on twinned single crystals can induce a motion of the twin boundary, so called 'detwinning' process. For a twinned single crystal with FM structure, the application of a magnetic field can also introduce stress which is generated through the Zeeman en-

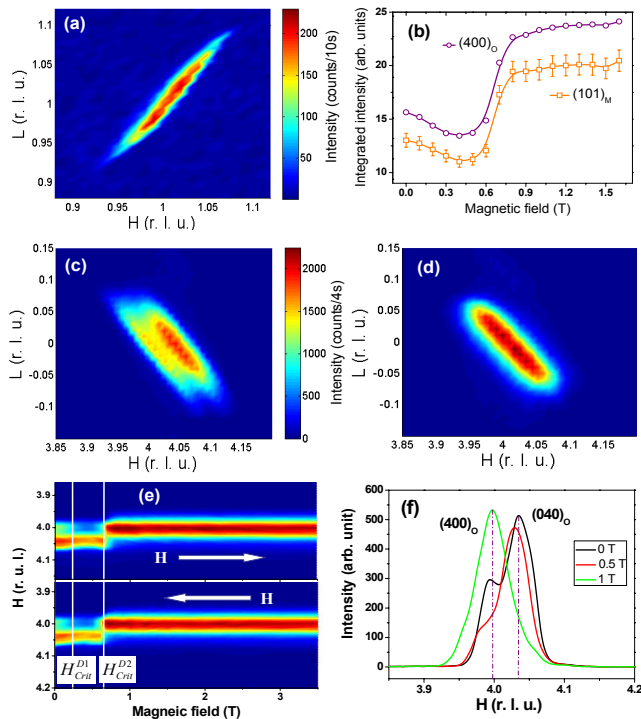


FIG. 4: (Color online) Selected Bragg reflections of EuFe_2As_2 at 2 K. (a) The contour map of $(101)_M$ reflection at 3 T field. (b) Field dependence of integrated intensities of $(400)_O$ and $(101)_M$ reflections. (c) and (d) The contour maps show the Q dependence of the $(400)_O$ and $(040)_O$ nuclear reflections at zero field and 3 T field, respectively. (e) Evolution of the distribution of $(400)_O$ and $(040)_O$ reflections with increasing and decreasing magnetic field at. (f) Q -scans of $(400)_O$ reflection under three typical magnitudes of magnetic field.

ergy $E = -\mu_0 \vec{M} \cdot \vec{H}$ and magnetic anisotropy energy. This detwinning process can be realized if the field induced stress is larger than the internal stress originated from twin dislocation. As illustrated in Fig. 3(b), the Eu spin rotates toward the a axis with increasing field. Concomitantly, the Zeeman energy decreases with increasing field strength and magnetization of the EuFe_2As_2 crystal. Thus, by minimizing the total energy, greater stress is generated and results in a single domain. Since the twinned structure only exist in the ab plane in present orthorhombic structure, the domain population does not change when a magnetic field is applied parallel to the c axis. Note that the twinned structure also plays a key role with respect to the magnetic and electric behaviors. For example, the in-plane resistivity can be affected remarkably by twin boundary scattering and the magnetization is associated with the response of different domains to the applied field. Since the twinning structure exhibits as the common feature for almost all orthorhombic phases in iron pnictides [18, 19], it is of great significant to detwin the crystals before performing various experiments to evaluate the real intrinsic properties.

Within the frame of the standard model for rare earth, the crystalline electric field (CEF) effect is responsible for the magnetic anisotropy for most of the rare earth ions with finite

orbital magnetic moment. However, for S -state rare earth ions, such as Gd^{3+} and Eu^{2+} , the CEF effect is negligible because of the vanishing of the orbital magnetic moment and the charge density is no longer coupled to the spin. Nevertheless, weak magnetic anisotropy is observed in both Gd^{3+} and Eu^{2+} contained compounds and the magnetic anisotropy is argued to be driven mainly by dipole-dipole interactions [20–22]. The magnetic anisotropy energy caused by the dipole-dipole interactions in EuFe_2As_2 was evaluated for three different ordered states of Eu^{2+} magnetic moments: ground state AFM configuration, FM configurations with moments aligned along a and c axes, respectively. By considering the contribution of neighboring magnetic atoms within the sphere of 25 Å radius, the dipolar energies are obtained to be $-206 \mu\text{eV}/\text{Eu}$, $-72 \mu\text{eV}/\text{Eu}$ and $158 \mu\text{eV}/\text{Eu}$ for above mentioned three ordered configurations, respectively. It clearly suggested that the dipolar interaction favors the AFM ordered state, while the hard axis is predicted to be c axis. Our experimental data are in good agreement with the prediction from the dipole-dipole interaction, which indicates a dominant contribution of the dipole-dipole interactions to the magnetic anisotropy of EuFe_2As_2 . Given the fact that the magnetization saturated at different fields for H parallel to the a and c axis due to the magnetic anisotropy [11], we argue that the magnetic anisotropy energy may also generate stress and be partly responsible for the movement of the twin boundaries under field.

In summary, our single crystal neutron diffraction experiments show a magnetic field induced magnetic phase transition in EuFe_2As_2 with the Eu moments changing from AFM to FM arrangement. The ordering temperature of the Eu moments increases with increasing field. Moreover, giant spin-lattice coupling has been observed as indicated by the redistribution of the domain population. Since the domain realignment is intimately correlated with the magnetic phase transition, the spin-lattice coupling in EuFe_2As_2 can be attributed to the stresses generated by Zeeman energy and magnetic anisotropy energy.

* y.xiao@fz-juelich.de

- [1] Y. Kamihara, T. Watanabe, M. Hirano, and H. Hosono, *J. Am. Chem. Soc.* **130**, 3296 (2008).
- [2] X. H. Chen, T. Wu, G. Wu, R. H. Liu, H. Chen, and D. F. Fang, *Nature (London)* **453**, 761 (2008).
- [3] M. Rotter, M. Tegel, and D. Johrendt, *Phys. Rev. Lett.* **101**, 107006 (2008).
- [4] C. de la Cruz, Q. Huang, J. W. Lynn, J. Li, W. Ratcliff II, J. L. Zarestky, H. A. Mook, G. F. Chen, J. L. Luo, N. L. Wang, and P. C. Dai, *Nature (London)* **453**, 899 (2008).
- [5] Q. Huang, Y. Qiu, W. Bao, J. W. Lynn, M. A. Green, Y. Chen, T. Wu, G. Wu, and X. H. Chen, *Phys. Rev. Lett.* **101**, 257003 (2008).
- [6] Y. Su, P. Link, A. Schneidewind, Th. Wolf, Y. Xiao, R. Mittal, M. Rotter, D. Johrendt, Th. Brueckel, and M. Loewenhaupt, *Phys. Rev. B* **79**, 064504 (2009).
- [7] I. I. Mazin, D. J. Singh, M. D. Johannes, and M. H. Du, *Phys.*

- Rev. Lett. **101**, 057003 (2008).
- [8] J. Zhao, Q. Huang, C. de la Cruz, S. Li, J. W. Lynn, Y. Chen, M. A. Green, G. F. Chen, G. Li, Z. Li, J. L. Luo, N. L. Wang, and P. Dai, *Nature Materials* **7**, 953 (2008).
- [9] C. Lester, Jiun-Haw Chu, J. G. Analytis, S. C. Capelli, A. S. Erickson, C. L. Condon, M. F. Toney, I. R. Fisher, and S. M. Hayden, *Phys. Rev. B* **79**, 144523 (2008).
- [10] Y. Xiao, Y. Su, M. Meven, R. Mittal, C.M.N. Kumar, T. Chatterji, S. Price, J. Persson, N. Kumar, S. K. Dhar, A. Thamizhavel, Th. Brueckel, *Phys. Rev. B* **80**, 174424 (2009).
- [11] Shuai Jiang, Yongkang Luo, Zhi Ren, Zengwei Zhu, Cao Wang, Xiangfan Xu, Qian Tao, Guanghan Cao and Zhu'an Xu, *New Journal of Physics* **11**, 025007 (2008).
- [12] T. Terashima, M. Kimata, H. Satsukawa, A. Harada, K. Hazama, S. Uji, H. S. Suzuki, T. Matsumoto, and K. Murata, *J. Phys. Soc. Jpn.* **78**, 083701 (2009).
- [13] Zhi Ren, Qian Tao, Shuai Jiang, Chunmu Feng, Cao Wang, Jianhui Dai, Guanghan Cao, and Zhu'an Xu, *Phys. Rev. Lett.* **102**, 137002 (2009).
- [14] H. S. Jeevan, Z. Hossain, Deepa Kasinathan, Helge Rosner, C. Geibel, and P. Gegenwart, *Phys. Rev. B* **78**, 092406 (2008).
- [15] Yanpeng Qi, Zhaoshun Gao, Lei Wang, Dongliang Wang, Xianning Zhang, and Yanwei Ma, *New Journal of Physics* **10**, 123003 (2008).
- [16] M. Chmielus, X. X. Zhang, C. Witherspoon, D. C. Dunand and P. Müllner, *Nature Materials* **8**, 863 (2009).
- [17] A. Sozinov, A. A. Likhachev, N. Lanska and K. Ullakko, *Appl. Phys. Lett.* **80**, 1746 (2002).
- [18] M. A. Tanatar, E. C. Blomberg, A. Kreyssig, M. G. Kim, N. Ni, A. Thaler, S. L. Bud'ko, P. C. Canfield, A. I. Goldman, I. I. Mazin, and R. Prozorov, arXiv:1002.3801.
- [19] Jiun-Haw Chu, James G. Analytis, Kristiaan De Greve, Peter L. McMahon, Zahirul Islam, Yoshihisa Yamamoto, and Ian R. Fisher, arXiv:1002.3364.
- [20] M. Colarieti-Tosti, S. I. Simak, R. Ahuja, L. Nordström, O. Eriksson, D. Åberg, S. Edvardsson, and M. S. S. Brooks, *Phys. Rev. Lett.* **91**, 157201 (2003).
- [21] Gerrit van der Laan, Elke Arenholz, Andreas Schmehl, and Darrell G. Schlom, *Phys. Rev. Lett.* **100**, 067403 (2008).
- [22] Samir Abdelouahed and M. Alouani, *Phys. Rev. B* **79**, 054406 (2009).